

Functional and microvascular anatomy of the ocular bulb in wild pig: a scanning electron microscopic study

Lutfi TAKCI^{1*}, İbrahim KÜRTÜL², Sadık YILMAZ³

¹Department of Anatomy, Faculty of Veterinary Medicine, Sivas Cumhuriyet University, Sivas, Turkey

²Department of Anatomy, Faculty of Medicine, Bolu Abant İzzet Baysal University, Bolu, Turkey

³Firat University, Faculty of Veterinary Medicine, Department of Anatomy, Elazığ, Turkey

Received: 18.11.2020 • Accepted/Published Online: 06.03.2021 • Final Version: 29.06.2021

Abstract: This study searched the functional, macro- and microvascular anatomy of the ocular bulb in the 20 wild pigs to evaluate the effects of domestication on the eye comparatively by applying macroanatomical dissection techniques, Crossmon's modified triple staining technique, and scanning electron microscopy (SEM) through corrosion cast technique. The ocular bulb was vascularized by the internal ophthalmic artery along with the external ophthalmic artery. Erythrocytes were observed in the capillaries of the inner layers of the retina. Distinctive functional adaptations were documented in the microvasculature of the ocular components, such as the marginal capillaries with irregular enlargements and narrowings following parallelly running and markedly convolute courses and ending with pinpoint-like terminations in the ciliary body. The iridal arterioles run a zigzag pathway, forming coherent undulations each other, and ending as bud-like structures, which seem to be artifacts due to incomplete filling of the resin. These peculiarities contribute probably to the compensation in capillary pressure.

Key words: Ocular bulb, corrosion cast, scanning electron microscopy (SEM), wild pig, vascularisation

1. Introduction

Pathological disorders can only be evaluated in reference to detail morphological knowledge of the vessels to the eyeball. With regard to that, detail vessel topography of this organ has amply been studied comparatively in several species including human [1, 2], monkey [3], horse [4], domestic pig [5], hamster [6], rat [7], rabbit [8], mouse [9], domestic farm animals, and peds [10,11]. The vascularization has been depicted in several species by the use of light [12], confocal [13], fluorescence [12,13], and scanning electron microscopes (SEMs) [4,12,13]. SEM is applied particularly through corrosion cast technic to describe microvascular peculiarities of the eyeball. Studies using this technique [5,7,10,11,14–16] have revealed a broad variation in structural and functional properties of the vessels such as diameters and sub-branch numbers in several animal models. They have thus provided very vital database for definition, diagnose, and treatment of the eyeball pathologies [4–6,17].

Eyeball of the domestic pig is very similar morphologically to that of the human being [18–22]. For this reason, its vascularization has been described previously [5] but, to date, no morphological study of the ocular

vasculature in the wild pig (*Sus scrofa*), believed as the wild ancestor of the domestic pig, is present in the literature yet. Therefore, this research has been conducted to report first detailed characterisation of the microvascular formation of the vessels in the eyeball of the wild pig, which has a wide range of living environment in Turkey. The results have comparatively been evaluated, and functional significance of the microvascularization has been discussed. The results will contribute surely to the formation of an eye model, which will be an essential tool in defining, diagnosing and treating eyeball pathologies in human being. They sure will also contribute to the microvascular anatomy of the vertebrate eye and serve as a reference for experimental eye research.

2. Materials and methods

Eyes of the 20 adult wild pigs (10 male and 10 female) hunted legally were examined for this study. They were dissected using macroanatomical dissection techniques, and were observed macroanatomically. In the study, eyes of 10 pigs were used for corrosion casting, and eyes of 10 pigs were used for examination under light microscope.

The cranial blood vessels were flushed with phosphate-buffered saline (PBS) solution at 37 °C right after

* Correspondence: lutfi_takci@hotmail.com

decapitation through the universally standard gray cannula (G:16G, external diameter: 1,8mm, length: 45mm, flow: 180ml/min, Novacath Medipro I.C.) inserted in the right and left common carotid arteries. Perfusion at manually oriented pressure, lasted until the completely clear solution emerging from the jugular veins. These arteries then were dissected peripherally throughout the origin of the right and left ophthalmic arteries. Subsequently, they were flushed with formaldehyde and Natrium chloride solutions, respectively by the same approach for fixation, using universally standard yellow cannula (G:24G, external diameter: 0,7mm, length: 19mm, flow: 20ml/min, Novacath Medipro I.C.). Then, these vessels were filled with nearly 2 mL methyl methacrylate-Mercox combination (Imicryl, Konya, Turkey) within one minute before the resin became solid under manually oriented pressure (approximately 120 mmHg) by again the same approach using a caulking gun, as indicated by the literature [23–25]. The time between decapitation and filling the vessels with the combination was nearly 10 h. The eyes were waited for 24 h at 40–60 °C for polymerization. After polymerization, they were macerated for 2–3 days by repeated baths in a 20% KOH solution at 50 °C, and were rinsed in tap water. No drying process was needed since the materials were already in solid condition. Each of the vascular casts was isolated and mounted on an aluminum stub, and then sputtered with gold in ion-coater (JEOL Ltd., Tokyo, Japan). The samples finally were examined by scanning electron microscopy, at 10kV accelerating voltage (JEOL JSM-5500LV, JEOL Ltd., Tokyo, Japan).

For light microscopy, the samples were fixed with 10% formaldehyde solution and were bathed in 70, 80, 96, and 100% ethyle alcohol series for one h. each. They were then embedded in paraffin and serially sectioned at 5–6 µm intervals. The slides were finally stained by the use of the modified Crossmon's triple staining technique [26,27]. They were examined through using a research microscope (Olympus BX50, Olympus Corporation Company, Tokyo, Japan). This study was approved by the Animal Experiments Local Ethics Committee of Mustafa Kemal University (MKU HADYEK; 2015/6-5).

3. Results

The external and internal ophthalmic arteries were the major arterial vessels supplying the eyeball (Figure 1). The former artery originated from the maxillary artery while the latter arose from the epidural rete mirabile and entered through the optic canal along with the optic nerve. In detail, 2 long posterior ciliary arteries following lateral and medial course, 2–4 short posterior ciliary arteries, and chorioretinal artery were responsible for the vascularisation of the eyeball (Figure 1, Figure 2). The long posterior ciliary arteries united, forming the major iridial arterial ring around the iris (Figure 1, Figure 2).

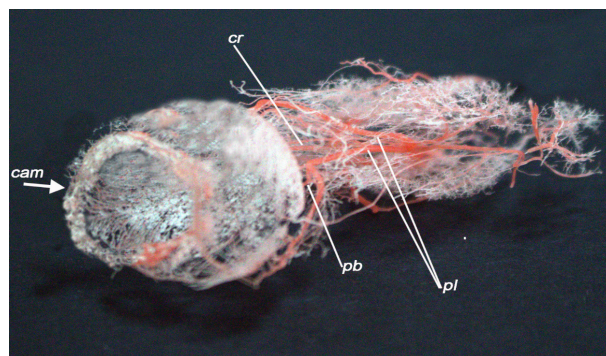


Figure 1. General view of the casts obtained from the ocular bulb (front view). Pl: long posterior ciliary artery, pb: short posterior ciliary artery, cr: chorioretinal artery, cam: major iridial arterial ring.

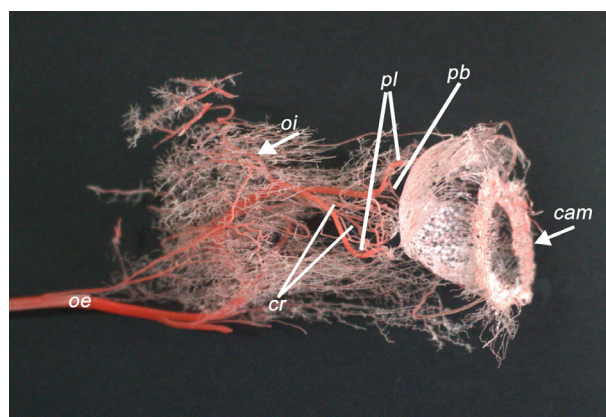


Figure 2. General view of the casts obtained from the ocular bulb (side view). Oe: external ophthalmic artery, oi: internal ophthalmic artery, pl: long posterior ciliary artery, pb: short posterior ciliary artery, cr: chorioretinal artery, cam: major iridial arterial ring.

The ciliary processes were supplied by the major iridial arterial ring. Capillaries of each ciliary process followed parallel and coiled courses (Figure 3). Nonuniform protrusions and narrowings were observed on the marginal capillaries (Figure 4). They ended by forming pinhead-like enlargements (Figure 3). Anastomoses were also observed between neighbouring marginal capillary plexuses (Figure 3). At histological views, the capillaries showed irregular distribution (Figure 5).

The iridial arterioles converged from the major iridial arterial ring, followed a zigzag pathway through the pupil, forming coherent undulations each other (Figure 6, Figure 7). Their terminal edges ended as bud-like structures, which seemed to be the artifacts. A prominent capillary network was seen around these vessels (Figure 6). A

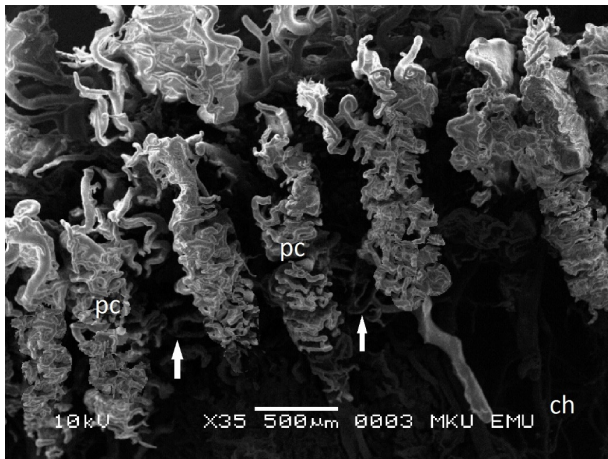


Figure 3. Capillary vessels of the ciliary process (SEM). pc: ciliary process marginal capillaries, ch: choroid, arrows: capillaries in ciliary process.

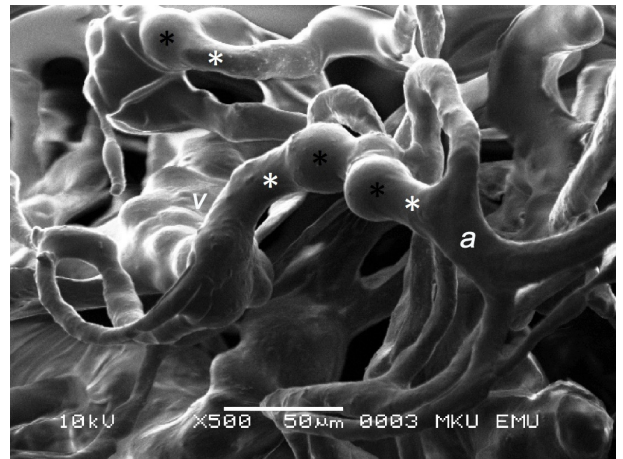


Figure 4. Irregular enlargement and narrowing of the marginal capillaries (SEM). Black asterisks: enlargements in the capillary lumen, white asterisks: narrowing in the capillary lumen, a: arteriole, v: venule.

narrowing was observed on the vessels of the capillary network, particularly at the orderly given subbranching sites (Figure 8). The orderly leaving branches out of the main vessel trunk dispersed with an almost 90° angle.

At histological level, the iridal arterioles were seen lying on a longitudinal pattern, following a spiral course (Figure 9). Several capillaries also encircled them (Figure 9).

The choroidal arteries originated from the short posterior ciliary artery with a 90° angle as several orderly leaving subbranches. There were nonuniform narrowings on the lumens of the arteries right at their origins as intra-arterial cushions (Figure 10). The choroid was the most vascularized component of the eyeball (Figure 10). The choroidal arteries followed straight parallel patterns through the anterior pole (Figure 10), interdigitating the densely packed choroidal veins draining the area (Figure

11, Figure 12). Anastomoses were observed between the arteries while no arterio-venous anastomose was determined (Figure 13).

The choroidal arteries ramified two or three times before becoming precapillary arterioles forming the capillary networks (Figure 10, Figure 11). The precapillary arterioles were larger in diameter, running a very short course, as compared to those in retina (Figure 12). The capillaries were homogeneously distributed, sinusoid-like structures, constructing very dense anastomoses in-between them and with the capillaries of the neighbouring precapillary arterioles (Figure 14, Figure 15).

Several blood vessels at various diameters were seen at light microscopic observations of the choroidea (Figure 16). Blood flow was through the enlargements at the

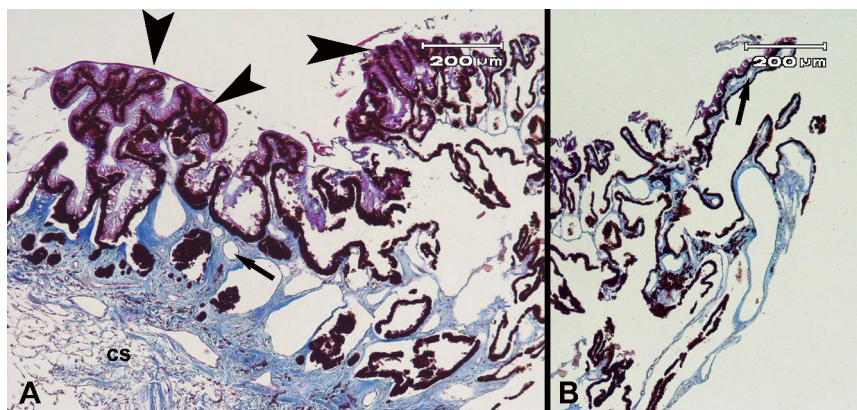


Figure 5. A. Histological image of the ciliary process. cs: ciliary body, arrows: ciliary process capillaries, arrowheads: ciliary part of the retina. B. Arrow: ciliary process capillaries.

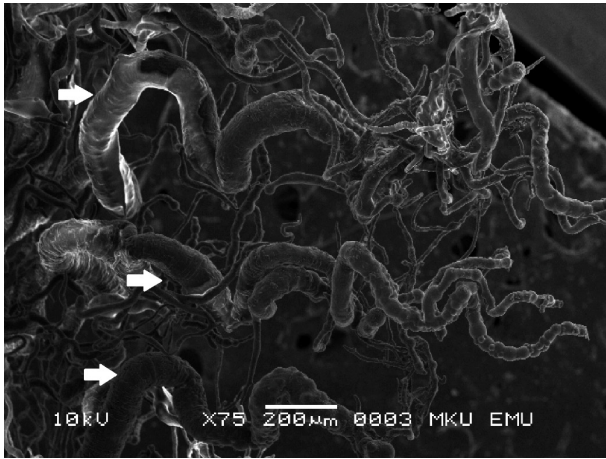


Figure 6. Vascularization of the iris (SEM). Arrows: vessels of the iris that zigzag towards the pupilla.

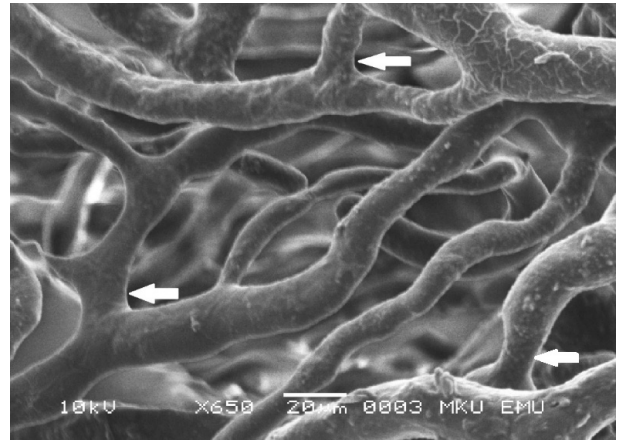


Figure 8. Iris capillaries (SEM). Arrows: narrowing in the branching areas.



Figure 7. Vessel endings in the vascularization of the iris (SEM). The terminal edges ended as bud-like structures which seemed to be the artifacts.

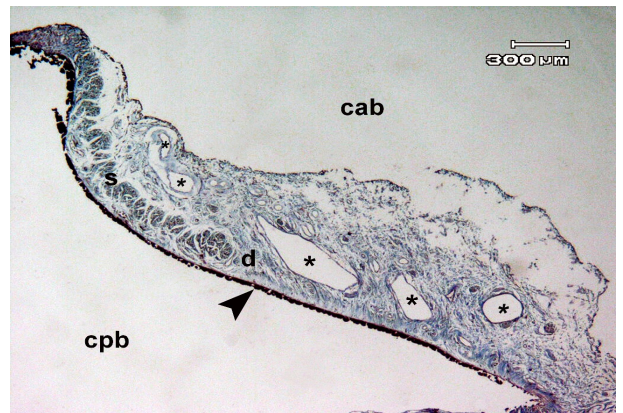


Figure 9. Histological image of the iris vascularization. cab: anterior chamber, cpb: posterior chamber, s: pupillary sphincter muscle, d: pupillary dilator muscle, asterisks: blood vessels, arrowhead: iridal part of the retina.

opening of the precapillary arterioles to the capillary beds (Figure 16).

The histological findings around the optic nerve entering the eyeball showed very dense vascularization (Figures 17, 18). The veins were characterized as possessing the lumens at larger diameter, thinner walls, and following loose and irregular patterns (Figure 17). Episcleral arteries and veins were prominent in the corneal limbus of the avascular cornea, and the scleral venous sinus (canal of Schlemm) was present at the corneoscleral junction (Figure 19).

The blood supply of the region of the retina closer to the choroidea was provided through the capillaries of the choroidea. The retina was holangiotoxic type possessing

a compact vessel network scattering throughout the light-sensitive portion of the retina. Blood flow in these capillary beds was through the enlargement areas at the levels of the precapillary vessels opening into the capillary beds (Figure 20). The shape of the capillary network seen in the avascular region of the retina was not present in the vascular region.

Histological findings of the retina revealed that neuroepithelial layer of the retina faced to diverge in all the slides (Figure 21). The other retinal layers were also determined histologically, showing clear vascularization (Figures 21). There were blood vessels lined under the internal limiting membrane of the retina (Figure 21). Erythrocytes were seen in the capillaries of the inner layers of the retina (Figure 22).

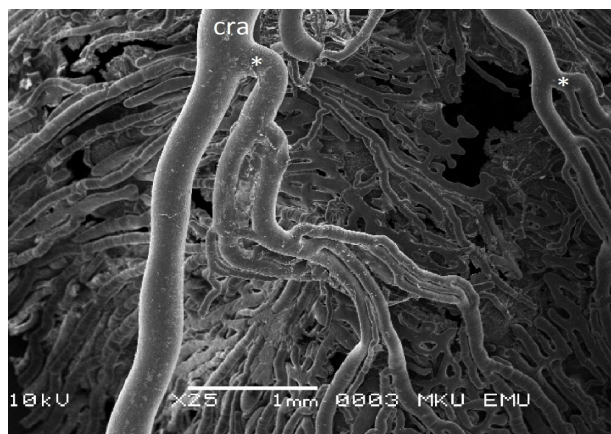


Figure 10. Vascularization of the choroid (SEM). cra: artery of the choroidea, asterisks: intra-arterial cushions seen in the branching areas (view from the outside of the ocular bulb).

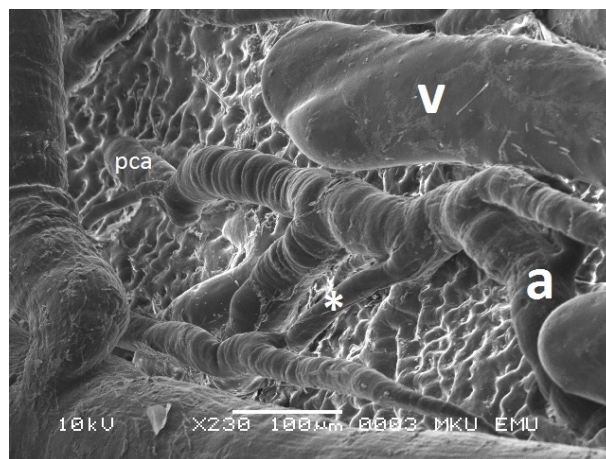


Figure 12. Vessels of the choroid (SEM). a: artery, v: vena, pca: precapillary artery, asterisk: artery-artery anastomosis (view from the outside of the ocular bulb).

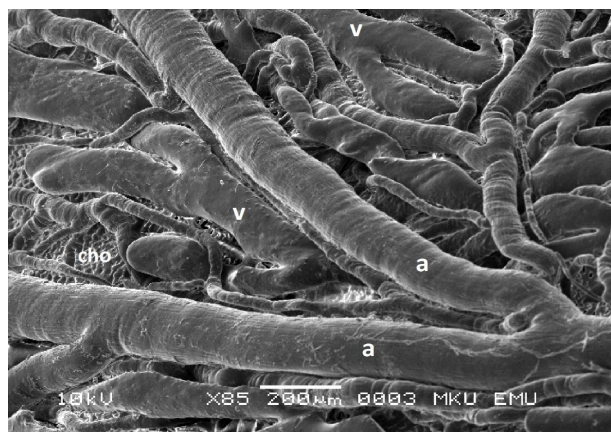


Figure 11. Choroidea arteries and veins (SEM). a: artery, v: vena, cho: choroid (view from outside of the ocular bulb).



Figure 13. Anastomoses in precapillary vessels (SEM). Asterisks: anastomoses between the arterioles.

4. Discussion

Filling of the vessels with the resin combination had certain difficulties during the application as the literature indicated [23–25]. Viscosity of the resin, pressure of the manual injection and time period between the death of the animal and casting were very important matters to concern. In other words, too viscous casting resin, inappropriate injection pressure and too late resin injection after the death of animal were the essential pitfalls of this method. Due to these, the resin filling procedure was applied right after the death and finished within the proper time period under manually oriented pressure (approximately 120 mmHg), as indicated by the literature. The whole method was practiced again and again to get proper manual skill.

The external ophthalmic artery supplied the eyeball mostly in the wild pig, depicted in Figures 1 and 2, as

indicated by the literature [4–6, 8, 9]. The artery sent off the short and long posterior ciliary arteries, and the chorioretinal artery just before entering the eyeball. As mentioned in the literature [18], since no central retinal artery is present in pig the chorioretinal artery has substituted this artery functionally, just as the case in our study.

The ciliary process acquires blood supply from the major iridial arterial ring formed by the long posterior

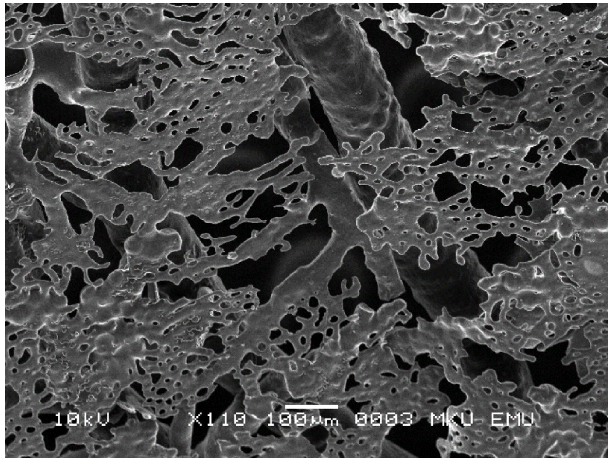


Figure 14. Vascularization of the choroid. Opening of precapillary vessels to capillary beds (SEM). (View from inside the ocular bulb).

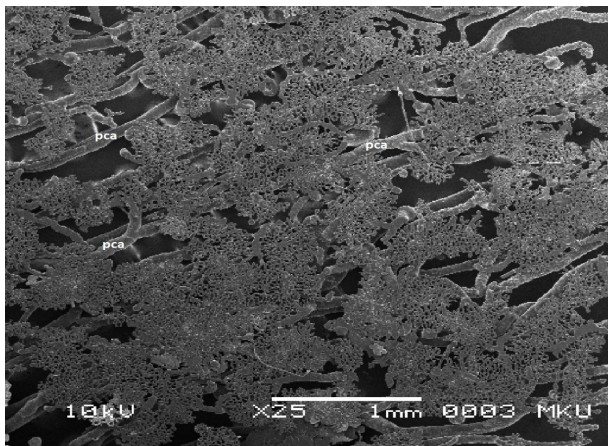


Figure 15. Capillaries of the choroid (SEM). pca: precapillary arterioles (view from inside the ocular bulb).

ciliary arteries in domestic pig, horse, rabbit, and rat [4,5,7,8] and by the anterior ciliary artery in hamster and mouse [6,9]. It was constituted by the long posterior ciliary arteries in the wild pig of our study, which is in parallel with the findings of the literature indicated above. The marginal capillaries regulate a ciliary capillary pressure to facilitate secretion of the aqueous humor. Similarly, our study has documented the massive ciliary vascular system in the wild pig as seen in Figure 3. In detail, irregular enlargements and narrowings in their diameters form thoroughfare channels to send the blood from the ciliary arterioles to the collecting venules, as displayed in the previous reports [4–6,8]. This is mostly for the regulation of the vascular resistance of the ciliary vessels; thus, enabling the secretion of the aqueous humor and contributing to a



Figure 16. Histological image of the choroid. s: sclera, c: choroidea, a: artery, v: vein.

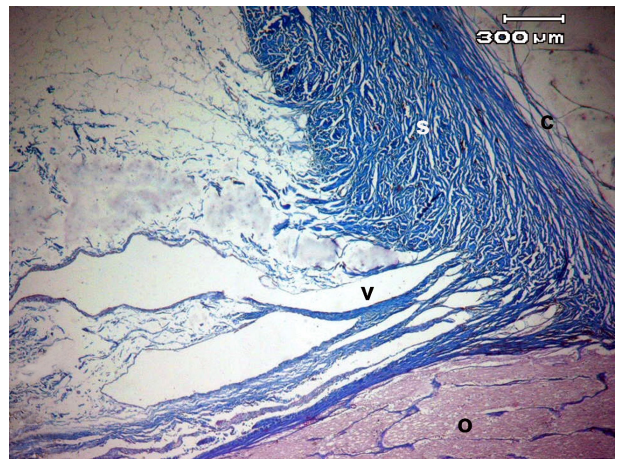


Figure 17. Histological image of the disc of the optic nerve. o: optic nerve, s: sclera, c: choroidea, v: vein.

system that compensates inner pressure of the eyeball. A similar morphology has also been observed in our study, as depicted in Figure 3, which is surely in relation directly to the ciliary body making humour aqueous.

Arterioles of the ciliary body have been shown to connect directly to the collecting venules [4–6,8]. These passages bypassing capillary system are observed in this study, indicating no difference between domestic and wild pigs and other animals.

The blood supply of the iris has been shown to converge from the major arterial circle, which is mostly similar to the reports in literature [4–6,8,9]. The narrowings observed particularly on the branching side as seen in Figure 8 and the orderly given subbranches dispersing from the parent artery with a 90° angle as shown in Figure 8 are very characteristic peculiarities, just as documented in other

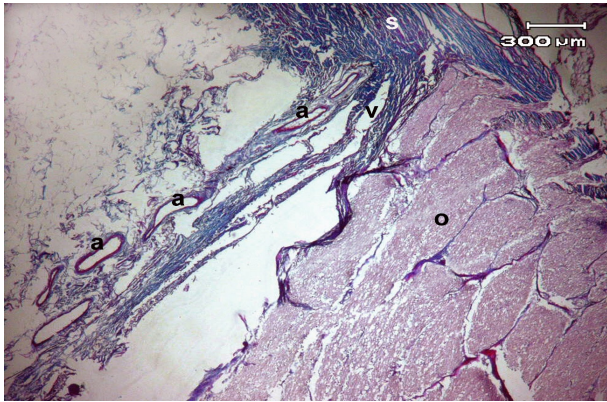


Figure 18. Histological image of the disc of the optic nerve. o: optic nerve, s: sclera, a: artery, v: vein.

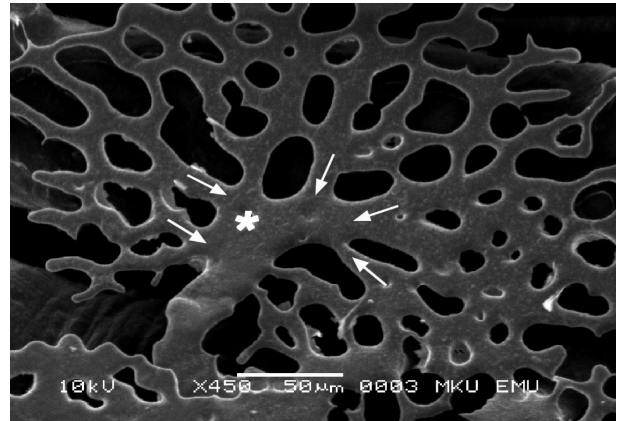


Figure 20. The choroidal region (SEM). Arrows: direction of blood flow, asterisk: enlarged region where the precapillary vessel opens into the capillary.

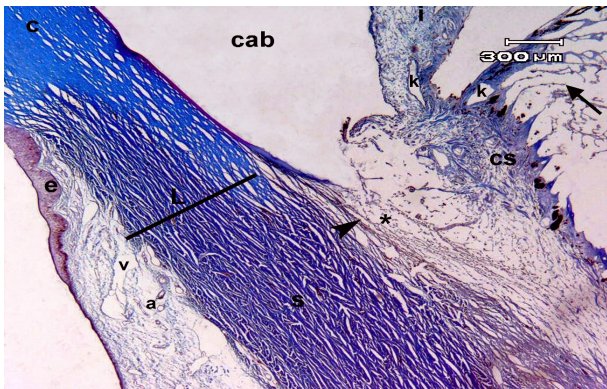


Figure 19. Histological image of the limbus region. L: limbus, s: sclera, c: cornea, cs: ciliary body, k: blood vessels, a: artery, v: vena, arrowhead: scleral venous sinus, arrow: zonular fibers, i: iris, e: layer of corneal epithelium, asterisk: trabecular mesh (Fontana slits), cab: anterior chamber.

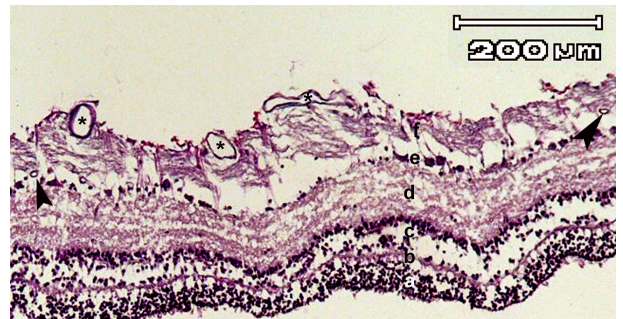


Figure 21. Histological image of the retina. a: outer nuclear layer, b: outer plexiform layer, c: inner nuclear layer, d: inner plexiform layer, e: ganglion cell layer, f: retinal nerve fibre layer; arrowheads: narrow-diameter capillary blood vessels in the inner layers of the retina, asterixes: blood vessels.

animals [4,10]. The course of the venules draining the iris shows similar pattern, as is the case in the literature [4–6]. The undulate courses of the iridal arterioles and venules have been indicated to be the results of the adaptation of the vessels to the accommodation of the pupil [4-9, 28, 29]. The bud-like structures observed on the terminal edges of the iridal arterioles displayed in Figure 7, have been reported neither in domestic pig nor in other animals. Even though we have repeated the trials with the best effort we can they seem to be the artifacts due mostly to insufficiently filled vessels characterized by the rounded tips that are observed when the hydrophobic resin used encounters with the rinsing solution.

Most of the vascularization of the choroidea is provided by the short posterior ciliary arteries by giving very short arterioles before constructing the capillaries [4,5,8]. Such course pattern and densely supply nature of

the arterioles as shown in Figure 10, are mostly in similar with the findings of previous studies indicated above. Likewise, the densely packed choroidal veins observed in this study follow similar blood flow as seen in the domestic pig and hamster [5,6] while the chorioretinal veins are the drainage point in the horse [4].

The visible difference between the diameters of arterioles and venules indicated in the literature [5,8] has also been seen in the wild pig as depicted in Figures 10,11,12. Yet, the shorter course and the larger diameter of the choroidal arterioles, as compared to the retinal arterioles, indicate faster blood flow, leading to higher blood pressure and higher permeability in the capillary networks of the choroid. This results in optimal nourishment of the retina through the filtration of the blood thereby. The densely packed capillary network and such microstructure in the choroid perfectly compensate the arterial blood pressure

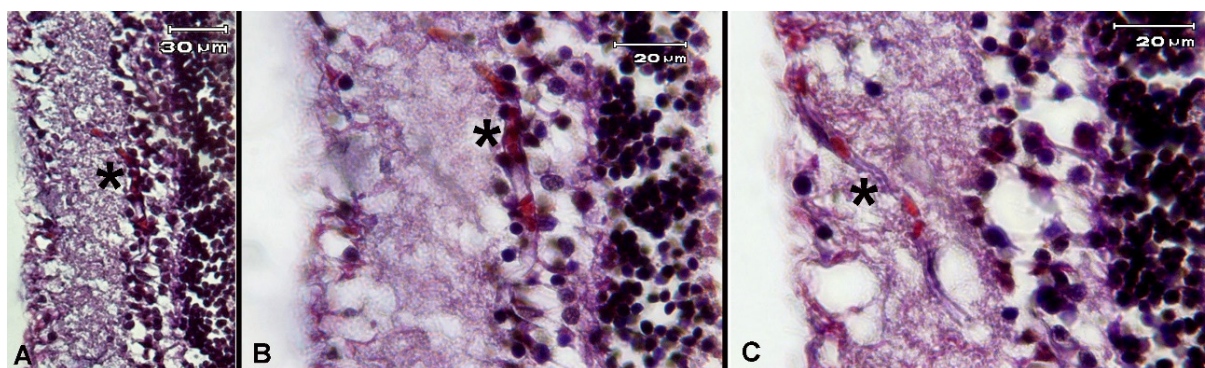


Figure 22. Blood vessels in the inner layers of the retina. Asterix: erythrocytes in blood vessels.

within the physiological levels in any case of the decrease at blood pressure to avoid a possible functional disorder in the retina. This study has also documented such a capillary system as seen in Figure 10. The limitless anastomoses observed in the capillary system of the choroid shown in Figure 13 indicate also a perfect balance system in the intraocular blood pressure in case of any obstruction.

Blood supply of the retina is provided by the chorioretinal artery and longitudinal pial vessels in domestic pig [5]. Diameters of the retinal capillaries formed by the retinal arterioles are so small that red blood cells can scarcely pass beyond. Our study has found that the central retinal artery lacks in the wild pig, and the chorioretinal artery instead is responsible for the nourishment of the retina, just as the case in the domestic pig. Thus, the component of the retina closer to the choroidea has been found to be supplied by the choroidal capillaries. Called as stars of Winslow shown the star-shaped, hexagonal structures have been seen in the avascular region in the wild pig. Direction of the blood flow in those capillaries is through the enlargement areas at the levels of the precapillary vessels opening into the capillary beds as seen in Figure 20. Further studies are needed to be conducted on the functional effect (s) of the presence of these beds in the avascular region only. It will be very interesting to reveal the functional results of such different nourishment of the retina.

Literature [5,7,30,31] has reported intra-arterial cushions formed by the thickening of the intima layer of the retinal and choroidal arterioles right at their origins. Functioning as the sphincters, they play very essential roles in the diminishing of blood flow downstream, thereby increasing intravasal pressure. Studies [5,32–34] have also indicated capillary subbranching with right angles and very small diameters, contributing surely to the plasma skimming in these capillaries. In our study, however, red blood cells have clearly been demonstrated histologically in the capillaries of the inner layers of the retina as displayed in Figure 22. This result is somehow

contrary to the conception that the intra-arterial cushions seen in the retinal and choroidal capillaries prevent the blood cells entering into the retina. Indeed, the cushions mostly block the blood cells but it is obvious from our results that this blockage is not at zero point.

In histological observations, a separation has been depicted in the neuroepithelial layer of the retina in all the slides as can be seen in Figure 21. This is due to the usage of the higher percentage of the formaldehyde (10 %) for fixation [35]. This literature suggests 4% paraformaldehyde or carbodiimide for fixation to avoid this separation. In our study, all the retina layers have been shown as displayed in Figure 21.

Histological studies on domestic pig have documented retinal arterioles and venules lying beneath the inner limiting membrane [36]. Similarly, optical coherence tomography has shown them at the same site in human being [37]. This study has also found similar results as demonstrated in Figure 21. Further to that, vessels with red blood cells have been documented in the other layers of the retina in this study as depicted in Figure 22. On the other hand, no such structure as Zinn–Haller circle seen in human being has been observed in the wild pig as is the case in rat, dog, monkey and domestic pig [1, 5].

Consequently, this study has documented that even though there is no macroscopical difference in the ocular circulation between domestic and wild pigs other than contribution of the small internal ophthalmic artery, histological and SEM observations have determined structural variations. Erythrocytes were observed in the capillaries of the inner layers of the retina. Distinctive functional adaptations have been seen in the microvasculature of the ocular components, including the marginal capillaries with irregular enlargements and narrowings that follow parallelly running and markedly convolute courses and ending with pinpoint-like terminations in the ciliary body. The iridal arterioles following a zigzag pathway and forming coherent undulations of each other are other adaptations

observed prominently. They probably contribute to the compensation in capillary pressure.

Acknowledgment

This study was performed for the PhD thesis of first author. The thesis study was supported by The Scientific and

Technological Research Council of Turkey (TUBITAK) Project No: 216S289

Ethical approval

This study was approved by The Animal Welfare Committee of Hatay Mustafa Kemal University (2015/6-5)

References

- Onda E, Cioffi GA, Bacon DR, van Buskirk EM. Microvasculature of the human optic nerve. *American Journal of Ophthalmology* 1995; 120 (1): 92-102.
- Krohn J, Bertelsen T. Corrosion casts of the suprachoroidal space and uveoscleral drainage routes in the human eye. *Acta Ophthalmol Scand* 1997; 75 (1): 32-35.
- Okada S, Ohta Y. Microvascular pattern of the retina in the Japanese monkey (*Macaca fuscata fuscata*). *Scanning Microscopy* 1994; 8 (2): 415-427.
- Ninomiya H, Inomata T. Functional microvascular anatomy of the horse eye: a scanning electron microscopic study of corrosion casts. *Open Journal of Veterinary Medicine* 2014; 4 (5): 91-101.
- Ninomiya H, Inomata T. Microvascular anatomy of the pig eye: scanning electron microscopy of vascular corrosion casts. *Journal of Veterinary Medical Science* 2006; 68 (11): 1149-1154.
- Ninomiya H, Inomata T. Microvasculature of the hamster eye: scanning electron microscopy of vascular corrosion casts. *Veterinary Ophthalmology* 2005; 8 (1): 7-12.
- Ninomiya H, Kuno H. Microvasculature of the rat eye: scanning electron microscopy of vascular corrosion casts. *Veterinary Ophthalmology* 2001; 4 (1): 55-59.
- Ninomiya H, Inomata T, Kanemaki N. Microvascular architecture of the rabbit eye: a scanning electron microscopic study of vascular corrosion casts. *Journal of Veterinary Medical Science* 2008; 70 (9): 887-892.
- Ninomiya H, Inomata T. Microvasculature of the mouse eye: scanning electron microscopy of vascular corrosion casts. *Journal of Experimental Animal Science* 2006; 43 (3): 149-59.
- Morrison JC, DeFrank M, Van Buskirk EM. Comparative microvascular anatomy of mammalian ciliary processes. *Investigative Ophthalmology & Visual Science* 1987; 28 (8): 1325-1340.
- Simoens P, Van den Broeck W, Lauwers H. Scanning electron microscopic study of the posterior ciliary veins in domestic ungulates. *Folia Morphologica-Warszawa-English Edition* 2001; 60 (1): 21-26.
- Aly K. *Glycohistochemical, Immunohistochemical and Electron Microscopic Examination of the Bovine Eyeball*: Imu. Munich, Germany: University Munich, 2003.
- Yu D, Yu P, Balaratnasingam C, Cringle S, Su E, et al. Microscopic structure of the retina and vasculature in the human eye. *Microscopy: Science, Technology, Applications and Education* 2010: 867-875.
- Bhutto IA, Amemiya T. Microvascular architecture of the rat choroid: corrosion cast study. *The Anatomical Record* 2001; 264 (1): 63-71.
- Morrison JC, Fraunfelder F, Milne ST, Moore CG. Limbal microvasculature of the rat eye. *Investigative Ophthalmology & Visual Science* 1995; 36 (3): 751-756.
- Morrison JC, Johnson EC, Cepurna WO, Funk RH. Microvasculature of the rat optic nerve head. *Investigative Ophthalmology & Visual Science* 1999; 40 (8): 1702-1709.
- Sugiyama K, Gu Z-B, Kawase C, Yamamoto T, Kitazawa Y. Optic nerve and peripapillary choroidal microvasculature of the rat eye. *Investigative Ophthalmology & Visual Science* 1999; 40 (13): 3084-3090.
- Prince JH, Diesem CD, Eglitis I, Ruskell G. *Anatomy and histology of the eye and orbit in domestic animals*. 1960.
- Bertschinger DR, Beknazar E, Simonutti M, Safran AB, Sahel JA, et al. A review of in vivo animal studies in retinal prosthesis research. *Graefes' Archive for Clinical and Experimental Ophthalmology* 2008; 246 (11): 1505-1517.
- Guduric-Fuchs J, Ringland LJ, Gu P, Dellett M, Archer DB, Cogliati T. Immunohistochemical study of pig retinal development. *Mol Vis*. 2009; 15: 1915-1928.
- Kivell TL, Doyle SK, Madden RH, Mitchell TL, Sims EL. An interactive method for teaching anatomy of the human eye for medical students in ophthalmology clinical rotations. *Anatomical sciences education* 2009; 2 (4): 173-8.
- Middleton S. Porcine ophthalmology. *Veterinary Clinics of North America: Food Animal Practice* 2010; 26 (3): 557-572.
- Hodde K, Steeber D, Albrecht R. Advances in corrosion casting methods. *Scanning microscopy*. 1990; 4 (3): 693-704.
- Minnich B, Lametschwandtner A. Scanning electron microscopy and vascular corrosion casting for the characterization of microvascular networks in human and animal tissues. *Microscopy: Science, Technology, Applications and Education*. 2010; 1: 29-39.

25. Verli FD, Rossi-Schneider TR, Schneider FL, Yurgel LS, de Souza MAL. Vascular corrosion casting technique steps. *Scanning*. 2007; 29 (3): 128-32.
26. Crossmon G. A modification of Mallory's connective tissue stain with a discussion of the principles involved. *The Anatomical Record*. 1937; 69 (1): 33-38.
27. Denk H, Künzele H, Plenk H, Rüschoff J, Seller W. *Romeis Mikroskopische Technik*. 17., neubearbeitete Auflage. Urban und Schwarzenberg, München-Wien Baltimore. 1989; 1: 439-450.
28. Morrison JC, DeFrank MP, Van Buskirk EM. Regional microvascular anatomy of the rabbit ciliary body. *Investigative ophthalmology & visual science*. 1987; 28 (8): 1314-1324.
29. Morrison JC, Van Buskirk EM. Ciliary process microvasculature of the primate eye. *American journal of ophthalmology*. 1984; 97 (3): 372-383.
30. Henkind P, De Oliveira LF. Retinal arteriolar annuli. *Investigative ophthalmology & visual science*. 1968; 7 (5): 584-591.
31. Casellas D, Dupont M, Jover B, Mimran A. Scanning electron microscopic study of arterial cushions in rats: A novel application of the corrosion-replication technique. *The Anatomical Record*. 1982; 203 (3): 419-428.
32. Fourman J, Moffat D. The effect of intra-arterial cushions on plasma skimming in small arteries. *The Journal of physiology*. 1961; 158 (2): 374-80.
33. Perkkiö J, Wurzinger L, Schmid-Schönbein H. Plasma and platelet skimming at T-junctions. *Thrombosis research*. 1987; 45 (5): 517-26.
34. Pannarale L, Onori P, Ripani M, Gaudio E. Precapillary patterns and perivascular cells in the retinal microvasculature. A scanning electron microscope study. *Journal of anatomy*. 1996; 188 (Pt 3): 693-703.
35. Ivanova E, Toychiev AH, Yee CW, Sagdullaev BT. Optimized protocol for retinal whole mount preparation for imaging and immunohistochemistry. *Journal of visualized experiments: JoVE*. 2013; (82): e51018.
36. Rootman J. Vascular system of the optic nerve head and retina in the pig. *The British journal of ophthalmology*. 1971; 55 (12): 808-819.
37. Campbell J, Zhang M, Hwang T, Bailey S, Wilson D, et al. Detailed vascular anatomy of the human retina by projection-resolved optical coherence tomography angiography. *Scientific reports*. 2017; 7: 4220.